HHS Public Access

Author manuscript

J Phys Chem Lett. Author manuscript; available in PMC 2016 July 07.

Published in final edited form as:

J Phys Chem Lett. 2016 January 7; 7(1): 111–116. doi:10.1021/acs.jpclett.5b02720.

Pulsed Dynamic Nuclear Polarization with Trityl Radicals

Guinevere Mathies, **Sheetal Jain**, **Marcel Reese**, and **Robert G. Griffin***

Francis Bitter Magnet Laboratory and Department of Chemistry, Massachusetts Institute of Technology, Cambridge, Massachusetts 02139, United States

Abstract

Continuous-wave (CW) dynamic nuclear polarization (DNP) is now established as a method of choice to enhance the sensitivity in a variety of NMR experiments. Nevertheless, there remains a need for the development of more efficient methods to transfer polarization from electrons to nuclei. Of particular interest are pulsed DNP methods because they enable a rapid and efficient polarization transfer that, in contrast with CW DNP methods, is not attenuated at high magnetic fields. Here we report nuclear spin orientation via electron spin-locking (NOVEL) experiments using the polarizing agent trityl OX063 in glycerol/water at a temperature of 80 K and a magnetic field of 0.34 T. ^{1}H NMR signal enhancements up to 430 are observed, and the buildup of the local polarization occurs in a few hundred nanoseconds. Thus, NOVEL can efficiently dynamically polarize ^{1}H atoms in a system that is of general interest to the solid-state DNP NMR community. This is a first, important step toward the general application of pulsed DNP at higher fields.

Graphical Abstract

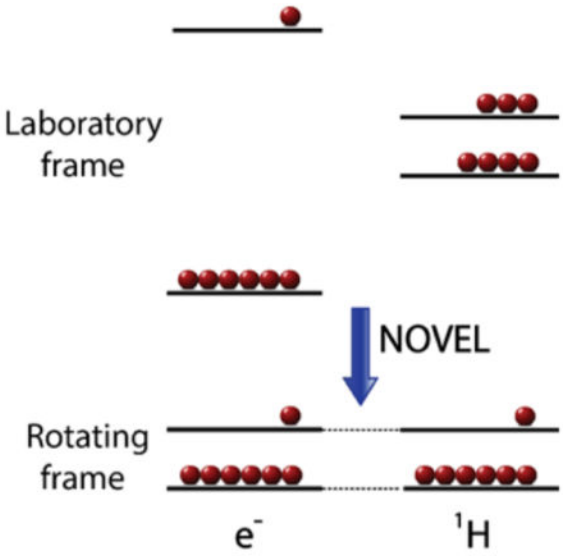

*Corresponding Author: rgg@mit.edu.

Notes

The authors declare no competing financial interest.

In dynamic nuclear polarization (DNP), electron spin polarization is transferred to nuclei via microwave irradiation at or near the electron Larmor frequency. DNP thereby enhances the nuclear spin polarization and can be used to increase the signal intensities in nuclear magnetic resonance (NMR) experiments. This requires the introduction of unpaired electrons into the NMR sample in the form of polarizing agents. When DNP and NMR experiments are performed at the same magnetic field and temperature, a maximum signal enhancement of $\gamma_e/\gamma_{1H} = 658$ can be achieved for protons, where γ_e and γ_{1H} are the gyromagnetic ratios of electrons and protons, respectively.

DNP is currently successfully utilized in a variety of NMR experimental protocols.[1–5] In magic-angle spinning (MAS) NMR, samples are dynamically polarized in situ, typically at temperatures of 80–100 K.[6–11] In contrast, in dissolution DNP, a static sample is polarized in a frozen, glassy matrix and subsequently melted with hot solvent such that solution NMR or MRI can be performed.[12–14] The mechanisms of DNP typically employed in these experiments are the cross-effect (CE)[15–18] and the solid-effect (SE).[19–23] Both of these mechanisms rely on state mixing from electron–nucleus interactions (as well as electron–electron interactions in case of the CE) in the laboratory frame and require continuous-wave (CW) microwave irradiation at high power to generate enhanced polarization of the nuclear spin manifold. Unfortunately, at higher magnetic fields the state mixing in the laboratory frame decreases due to the increasing strength of the electron and nuclear Zeeman terms, and the DNP efficiency attenuates as $\sim 1/B_0$ for the CE and $\sim 1/B_0^2$ for the SE. In MAS NMR experiments at higher fields (≥600 MHz/395 GHz) DNP enhancements are currently well below the theoretical maximum.[24–26] In dissolution DNP the detrimental field dependence is partially circumvented by performing DNP at 95 GHz (3.4 T or 144 MHz), followed by sample shuttling to higher field for the NMR experiment; however, as a consequence, polarization buildup is done at very low temperature, typically ~1.2 K, and the ^{13}C buildup times are very long, on the order of a few hours.[27,28]

While the detrimental field dependence is inherent to the CW DNP mechanisms SE and CE, it is possible to use other DNP mechanisms where the efficiency does not depend on the magnetic field. In particular, one can adapt approaches originally developed to detect low-γ nuclei in time-domain NMR experiments such as INEPT in solution[29] and cross-polarization in solids.[30,31] In these methods, energy level degeneracy, and thereby strong state mixing, is created in the rotating frame by the application of microwave and RF pulses. The Hamiltonian in the rotating frame contains no Zeeman terms and therefore the state mixing is not decreased at high magnetic fields. Moreover, there is the additional benefit that, compared with high-power CW microwave radiation, generating high-power microwave pulses is technically less challenging.

To date, several forms of pulsed DNP have been proposed. These include DNP in the nuclear rotating frame,[32,33] the dressed state solid effect (DSSE),[34,35] polarization of nuclear spins enhanced by ENDOR (PONSEE),[36,37] and nuclear spin orientation via electron spin locking (NOVEL).[38–40] In this last scheme, which is based on the method of cross-polarization, polarization is efficiently transferred from electrons to nuclei using a rotating frame/lab frame Hartmann–Hahn matching condition $\omega_{1S} = \omega_{0I}$, where $\omega_{1S} = \gamma_e B_1$ is the electron Rabi frequency and $\omega_{0I} = \gamma_n B_0$ is the nuclear Larmor frequency.

The initial NOVEL experiments reported at ≤0.34 T or 15 MHz were performed on a single crystal of silicon doped with boron acceptors[40] and later in diamond.[41] In both cases the enhancements were small and the buildup of polarization was limited by the slow spin diffusion in the ^{29}Si or ^{13}C spin reservoirs; however, the low Larmor frequencies of these two spin species facilitated satisfying the NOVEL matching condition. Very recently NOVEL was employed to polarize bulk ^{1}H, and because of improvements in instrumentation and sample preparation the enhancements were larger. Enhancements of 163 and 323 were observed in a single crystal of benzophenone doped with diphenylnitroxide and in partially deuterated polystyrene doped with BDPA, respectively.[42] In single crystals of naphthalene doped with pentacene,[43–47] *p*-terphenyl doped with pentacene,[48] and fluorene doped with acridine,[49,50] NOVEL has been used in combination with the integrated solid effect (ISE) to transfer polarization from photoexcited triplet states to ^{1}H.[51] Because of the non-Boltzmann polarization of these photoexcited triplet states, enhancements $>\gamma_e/\gamma_{1H}$ were obtained in these experiments.

Here we report NOVEL experiments using the polarizing agent trityl OX063 in a glycerol/water matrix at a temperature of 80 K and a magnetic field of 0.34 T. This highly stable radical is widely used in MAS DNP, dissolution DNP, and in vivo oxygen/EPR imaging.[12,52] The glycerol/water matrix facilitates application of NOVEL to biological structures by sample doping with trityl, similar to doping with biradicals in current CE MAS DNP.[7,53–56] The ^{1}H NMR signal enhancements we obtain are large, up to 430, and the buildup of bulk ^{1}H hyperpolarization is rapid, <8 s.

A description of the polarization transfer in NOVEL from a single unpaired electron (S = 1/2) to a single proton (I = 1/2) requires the following Hamiltonian in the rotating frame[57]

$$H=\Delta\hat{S}_z-\omega_{01H}\hat{I}_z+A_{zx}\hat{S}_z\hat{I}_x+A_{zy}\hat{S}_z\hat{I}_y+A_{zz}\hat{S}_z\hat{I}_z+\omega_{1S}\hat{S}_x \quad (1)$$

where $\Delta = \omega_{0S} - \omega_{\mu w}$ with ω_{0S} the electron Larmor frequency and $\omega_{\mu w}$ the microwave frequency. The other terms are the nuclear Zeeman term, the secular and pseudosecular hyperfine interaction with a nearby proton, and the microwave irradiation, respectively. An approximate energy level degeneracy is created when the electrons are spin-locked by on-resonance microwave irradiation ($\Delta = 0$) with a field strength of ω_{01H}. Strong state mixing then arises from the pseudosecular terms of the proton hyperfine interaction (i.e., the dipolar interaction), which is on the order of a megahertz for trityl OX063.[58,59]

Figure 1 shows 15 MHz ^{1}H NMR spectra of a 50 μL sample of d_8-glycerol/D_2O/H_2O 60:30:10 v/v/v doped with 10.5 mM trityl OX063 acquired with the NOVEL sequence “on” and “off”. (See the Experimental Methods section for a detailed description of the experimental protocol.) Acquisition of the off-signal with a sufficiently high signal-to-noise ratio requires ~12 h, whereas acquisition of the on-signal consumes ~15 min. The enhancement, $\varepsilon = (I_{on}/I_{off}) - 1$, with the NOVEL sequence on is 380 (±50). The phase of the on-signal is opposite to the phase of the off-signal, which is due to the choice of the phase of the electron spin locking pulse relative to the 90° flip pulse (see Scheme 1).[42] The on-

spectrum shows a central peak of a fwhm (full width at half-maximum) of ~15 kHz, which is typical for protons in this solid matrix,[60] and two shoulders, which are offset with respect to the central peak by roughly 50 kHz. Possibly these shoulders arise from protons that interact with the unpaired electron on trityl.

Figure 2 shows the enhancement of the ^{1}H NMR signal as a function of the length of the locking pulse (mixing time). The transfer of polarization from the electron to protons is nearly complete after ~300 ns. After the initial rise the enhancement drops slightly and transient oscillations are present in the curve, reflecting the coherent nature of the polarization transfer. Similar oscillations have been observed in ^{1}H–^{13}C cross-polarization experiments in a ferrocene single crystal[61] as well as in NOVEL experiments on single crystals.[49,50] For our system the oscillations are expected to be attenuated by the powder averaging and because electron–nuclear dipolar interactions occur with many different protons located both on the trityl molecule and in the solvent.[58,59]

Figure 3 shows the enhancement of the ^{1}H NMR signal as a function of the applied microwave field strength, $\gamma_e B_1$ (in MHz), and we consequently refer to this figure as a microwave field profile. The enhancement reaches a maximum around 15 MHz. Thus, the polarization transfer is most efficient at the NOVEL condition $\gamma_e B_1 = \gamma_n B_0$. The fwhm of the microwave field profile is 6 MHz, which roughly corresponds to the fwhm of the central peak in the echo-detected EPR spectrum of trityl OX063, which is 7 MHz, shown in Figure 4. Above $\gamma_e B_1 \approx 20$ MHz a significant enhancement of about~ 15% of the maximum remains. This is presumably due to higher order effects.[47]

Figure 4 shows the NOVEL enhancement Zeeman field profile together with the echo-detected EPR spectrum of the same sample. The central peak in the field profile is wider than the central peak in the EPR spectrum: fwhm = 20 MHz as opposed to 7 MHz (0.1 mT = 2.8 MHz). Thus, NOVEL occurs even when the microwaves are off resonance ($\Delta \neq 0$). In this case the nutation frequency of the electrons is given by $\omega_{\text{eff}} = (\Delta^2 + \omega_{1S}^2)^{1/2}$, where $\omega_{1S} \approx 2\pi \times 15$ MHz. The small contribution of Δ makes the NOVEL matching condition relatively broad. Remarkably, when going further off-resonance, both above and below the central peak, the enhancement does not decay to zero but remains ~10% of the maximum enhancement on resonance. (Note that around 348.35 mT the phase of the enhanced ^{1}H NMR signal is inverted.) Also, two side peaks are observed, one positive around 349.9 mT and one negative around 348.0 mT. We suspect that in these far-off-resonance regions second-order terms give rise to a small transfer of polarization.

The echo-detected EPR spectrum of trityl OX063 in Figure 4 also exhibits two sidebands, separated roughly 15 MHz from the central peak. In EPR spectra of low concentration trityl samples (≤0.2 mM) “spin-flip” lines, which are due to forbidden hyperfine transitions, are observed at these field positions;[62] however, the intensity of these spin-flip lines is much smaller than the intensity of the sidebands in our spectrum. This might be related to the high trityl concentration in our DNP samples, 10.5 mM for the sample in Figure 4. Recently trityl OX063 has been shown to aggregate in aqueous solutions at concentrations >1 mM.[63] We performed NOVEL experiments with various concentrations of trityl and found that the enhancements increase roughly up to 10 mM. At higher concentrations the echo-detected

EPR spectra are strongly distorted, presumably due to aggregation effects, and enhancements decrease.

The number of electrons in our sample is much smaller than the number of protons to be polarized. Thus, polarization of bulk protons requires nuclear spin diffusion.[64] The buildup of this hyperpolarization takes much longer than the initial polarization transfer from electron to nearby proton.[65] We measured this buildup time, T_B, on a sample that contained 6.4 mM to be 7.6 s. Note that this is much shorter than the nuclear T_1, which we found to be 26 s on the same sample.

To "pump" the proton polarization as efficiently as possible, we should maximize the repetition rate of the lock pulse sequence during bulk-polarization buildup. This rate is currently limited by the duty cycle of the TWT amplifier, which is 1%, and the electronic longitudinal relaxation time, T_{1e}, of trityl. On a sample containing 6.4 mM trityl OX063 we measured T_{1e} via inversion recovery to be 2.1 ms. For this same sample a lock sequence repetition time of 1 ms was found to yield the optimal enhancement.

In NMR a flip-back pulse of phase $-x$ after a spin-lock period can be used to bring the magnetization back along z, either for prolonged storage or to allow a shorter recycle delay between acquisitions.[66] In our NOVEL experiments a flip-back pulse immediately after the electron spin lock shortens the optimal shot-repetition time for the lock pulses to 0.5 ms, and, moreover, it increases the final enhancement by 15%.

What makes trityl OX063 such an efficient polarizing agent for NOVEL? (i) The EPR spectrum of trityl in frozen solution is very narrow. In our sample the central line has an fwhm of 7 MHz. This allows efficient excitation of all electrons in the sample with a 16 ns 90° pulse (corresponding to a bandwidth of 63 MHz). (ii) Trityl OX063 and its relatives were designed to minimize the isotropic hyperfine interaction with protons. At the same time there are many protons close enough to the unpaired electron to allow a strong dipolar interaction, that is, protons on the $–CH_2–$ groups and in the solvent.[58,59] All trityl radicals contribute efficiently to DNP at the NOVEL condition $\gamma_e B_1 = \gamma_n B_0$. (iii) Trityl OX063 has a very small g-anisotropy and a relatively long T_{1e},[67] which allows efficient spin-locking. On the other hand, the electronic T_{1e} is not too long to prohibit fast repetition of the locking sequence.

In conclusion, our experiments show that NOVEL can very efficiently polarize protons in a system that is of general interest to the solid-state DNP NMR community. This is a first, important step toward the general application of pulsed DNP at higher fields. Future work would include the development of high-frequency microwave sources that are able to generate the high-power pulses necessary to perform electron spin locking at higher fields.[68,69] At W band (95 GHz/3.4 T/144 MHz), amplifiers capable of producing kilowatt microwave pulses are already commercially available, and with a specialized setup NOVEL DNP at this frequency seems within reach. In addition one could think of alternative pulsed DNP methods, for which trityl OX063 in a frozen glycerol/water matrix is a good model system.

EXPERIMENTAL METHODS

NMR/EPR/DNP experiments at 15 MHz/9.8 GHz were performed on a Bruker ElexSys E580 X-band EPR spectrometer using an EN 4118X-MD4 (ENDOR) probe containing a dielectric microwave resonator. Microwave pulses were amplified using a 1 kW TWT amplifier 117X (Applied Systems Engineering, Fort Worth, TX). The ENDOR RF coil was tuned with an external tuning-matching circuit. NMR signals were detected with an iSpin-NMR System (SpinCore Technologies) with RF pulses amplified using a 1000 W LPI-10-21001 linear pulse amplifier (ENI, Rochester, NY). The sample temperature was kept at 80 K using a CF 935 flow cryostat with liquid nitrogen as a cryogen and an ITC 503S temperature controller (Oxford Instruments).

Solid-state ^{1}H NMR signals were acquired using a solid echo pulse sequence $(\pi/2)_X - \tau - (\pi/2)_Y - t - echo -$ with 90° pulses of 2.5 μs and t = 20 μs, with the phases of the pulses cycled through the conventional eight steps. Proton–proton dipole couplings lead to a short nuclear T_2 in our sample. Each acquisition consisted of 128 points and was performed with a detection bandwidth of 1 MHz. The signal was zero filled up to 1024 points prior to Fourier transformation.

Echo-detected EPR spectra were obtained using a Hahn echo pulse sequence $(\pi/2)_X - t - (\pi)_X - t - echo -$ with 90° pulses of 16 ns and t = 500 ns using a two-step phase cycle. At each field position 100 acquisitions were performed with a repetition rate of 1 kHz. To record the echo intensity we set the integration window to cover the entire echo. Rise and fall time of the microwave pulses is ~2 ns.

NOVEL experiments were performed at the magnetic field that gave the strongest EPR echo intensity. The NOVEL pulse sequence is shown in Scheme 1. A presaturation sequence consisting of 16 120° pulses 10 ms apart is used to remove previously existing nuclear polarization. Subsequently, polarization is built up by running the NOVEL sequence for several seconds with a repetition rate of 1 kHz. The microwave cavity is maximally overcoupled, and the microwave power attenuation was set to 8 dB to generate a $\gamma_e B_1$ field of 15.6 MHz (corresponding to a 90° pulse of 16 ns) to fulfill the NOVEL condition. The length of the lock pulse was generally set to 500 ns. After hyperpolarization buildup an NMR experiment is performed. NMR signal enhancements by NOVEL were determined by comparing the spectral intensities of the on and off signals.

Samples for DNP experiments contained ~10 mM trityl OX063 in d_8-glycerol/D_2O/H_2O 60/30/10 v/v/v (a.k.a. “DNP juice”) with 1 M urea.[70] Exact trityl concentrations were determined by UV–vis absorption spectroscopy. Thin-wall precision quartz EPR sample tubes with an OD of 4 mm were used (Wilmad-LabGlass), which were filled to a sample volume of 50 μL.

Acknowledgments

This research was supported by the National Institutes of Biomedical Imaging and Bioengineering through grants EB-002026 and EB-002804. G.M. gratefully acknowledges the support of a Rubicon Fellowship from The Netherlands Organization for Scientific Research (NWO). In addition, we gratefully acknowledge stimulating discussions with Prof. Björn Corzilius and Dr. Albert A. Smith.

References

1. Maly T, Debelouchina GT, Bajaj VS, Hu KN, Joo CG, Mak–Jurkauskas ML, Sirigiri JR, van der Wel PCAvd, Herzfeld J, Temkin RJ, Griffin RG. Dynamic nuclear polarization at high magnetic fields. J Chem Phys. 2008; 128:052211. [PubMed: 18266416]
2. Griffin RG, Prisner TF. High field dynamic nuclear polarization–the renaissance. Phys Chem Chem Phys. 2010; 12(22):5737–5740. [PubMed: 20485782]
3. Ni QZ, Daviso E, Can TV, Markhasin E, Jawla SK, Swager TM, Temkin RJ, Herzfeld J, Griffin RG. High frequency dynamic nuclear polarization. Acc Chem Res. 2013; 46(9):1933–1941. [PubMed: 23597038]
4. Can TV, Ni QZ, Griffin RG. Mechanisms of dynamic nuclear polarization in insulating solids. J Magn Reson. 2015; 253:23–35. [PubMed: 25797002]
5. Ardenkjaer-Larsen JH, Boebinger GS, Comment A, Duckett S, Edison AS, Engelke F, Griesinger C, Griffin RG, Hilty C, Maeda H, Parigi G, Prisner T, Ravera E, van Bentum J, Vega S, Webb A, Luchinat C, Schwalbe H, Frydman L. Facing and Overcoming Sensitivity Challenges in Biomolecular NMR Spectroscopy. Angew Chem, Int Ed. 2015; 54(32):9162–9185.
6. Mak-Jurkauskas ML, Bajaj VS, Hornstein MK, Belenky M, Griffin RG, Herzfeld J. Energy transformations early in the bacteriorhodopsin photocycle revealed by DNP-enhanced solid-state NMR. Proc Natl Acad Sci U S A. 2008; 105(3):883–888. [PubMed: 18195364]
7. Bajaj VS, Mak-Jurkauskas ML, Belenky M, Herzfeld J, Griffin RG. Functional and shunt states of bacteriorhodopsin resolved by 250 GHz dynamic nuclear polarization–enhanced solid-state NMR. Proc Natl Acad Sci U S A. 2009; 106:9244–9249. [PubMed: 19474298]
8. Lesage A, Lelli M, Gajan D, Caporini MA, Vitzthum V, Miéville P, Alauzun J, Roussey A, Thieuleux C, Mehdi A, Bodenhausen G, Copéret C, Emsley L. Surface Enhanced NMR Spectroscopy by Dynamic Nuclear Polarization. J Am Chem Soc. 2010; 132:15459–15461. [PubMed: 20831165]
9. Rosay M, Tometich L, Pawsey S, Bader R, Schauwecker R, Blank M, Borchard PM, Cauffman SR, Felch KL, Weber RT, Temkin RJ, Griffin RG, Maas WE. Solid-state dynamic nuclear polarization at 263 GHz: spectrometer design and experimental results. Phys Chem Chem Phys. 2010; 12(22): 5850–5860. [PubMed: 20449524]
10. Bayro MJ, Debelouchina GT, Eddy MT, Birkett NR, MacPhee CE, Rosay M, Maas WE, Dobson CM, Griffin RG. Intermolecular Structure Determination of Amyloid Fibrils with Magic-Angle Spinning and Dynamic Nuclear Polarization NMR. J Am Chem Soc. 2011; 133:13967–13974. [PubMed: 21774549]
11. Barnes AB, Markhasin E, Daviso E, Michaelis VK, Nanni EA, Jawla SK, Mena EL, DeRocher R, Thakkar A, Woskov PP, Herzfeld J, Temkin RJ, Griffin RG. Dynamic nuclear polarization at 700 MHz/460 GHz. J Magn Reson. 2012; 224:1–7. [PubMed: 23000974]
12. Ardenkjaer-Larsen JH, Fridlund B, Gram A, Hansson G, Hansson L, Lerche MH, Servin R, Thaning M, Golman K. Increase in signal-to-noise ratio of > 10,000 times in liquid-state NMR. Proc Natl Acad Sci U S A. 2003; 100(18):10158–10163. [PubMed: 12930897]
13. Golman K, Ardenkjaer-Larsen JH, Petersson JS, Mansson S, Leunbach I. Molecular imaging with endogenous substances. Proc Natl Acad Sci U S A. 2003; 100(18):10435–10439. [PubMed: 12930896]
14. Bowen S, Hilty C. Time-resolved dynamic nuclear polarization enhanced NMR spectroscopy. Angew Chem, Int Ed. 2008; 47(28):5235–5237.
15. Kessenikh AV, Lushchikov VI, Manenkov AA, Taran YV. Proton polarization in irradiated polyethylenes. Sov Phys Solid State. 1963; 5:321–329.
16. Kessenikh AV, Manenkov AA, Pyatnitskii GI. On explanation of experimental data on dynamic polarization of protons in irradiated polyethylenes. Sov Phys Solid State. 1964; 6:641–643.
17. Hwang CF, Hill DA. Phenomenological model for the new effect in dynamic polarization. Phys Rev Lett. 1967; 19:1011–1014.
18. Hwang CF, Hill DA. New effect in dynamic polarization. Phys Rev Lett. 1967; 18:110–112.
19. Jeffries CD. Polarization of Nuclei by Resonance Saturation in Paramagnetic Crystals. Phys Rev. 1957; 106(1):164–165.

20. Abragam A, Combrisson J, Solomon I. Polarisation Dynamique Des Noyaux Du Silicium 29 Dans Le Silicium a 4,2-Degrees-K. Cr Hebd Acad Sci. 1958; 247(25):2337–2340.
21. Erb E, Motchane JL, Uebersfeld J. Sur Une Nouvelle Methode De Polarisation Nucleaire Dans Les Fluides Adsorbes Sur Les Charbons - Extension Aux Solides Et En Particulier Aux Substances Organiques Irradiees. Cr Hebd Acad Sci. 1958; 246(21):3050–3052.
22. Shimon D, Feintuch A, Goldfarb D, Vega S. Static H-1 dynamic nuclear polarization with the biradical TOTAPOL: a transition between the solid effect and the cross effect. Phys Chem Chem Phys. 2014; 16(14):6687–6699. [PubMed: 24585094]
23. Shimon D, Hovav Y, Feintuch A, Goldfarb D, Vega S. Dynamic nuclear polarization in the solid state: a transition between the cross effect and the solid effect. Phys Chem Chem Phys. 2012; 14(16):5729–5743. [PubMed: 22419272]
24. Koers EJ, van der Cruijsen EA, Rosay M, Weingarth M, Prokofyev A, Sauvee C, Ouari O, van der Zwan J, Pongs O, Tordo P, Maas WE, Baldus M. NMR-based structural biology enhanced by dynamic nuclear polarization at high magnetic field. J Biomol NMR. 2014; 60(2–3):157–168. [PubMed: 25284462]
25. Kaplan M, Cukkemane A, van Zundert GCP, Narasimhan S, Daniels M, Mance D, Waksman G, Bonvin AMJJ, Fronzes R, Folkers GE, Baldus M. Probing a cell-embedded Megadalton protein complex by DNP-supported solid-state NMR. Nat Methods. 2015; 12:649–652. [PubMed: 25984698]
26. Frederick KK, Michaelis VK, Corzilius B, Ong T, Jacavone A, Griffin RG, Lindquist S. Sensitivity-Enhanced NMR Reveals Alterations in Protein Structure by Cellular Milieus. Cell. 2015; 163:620–628. [PubMed: 26456111]
27. Comment A, van den Brandt Bvd, Uffmann K, Kurdzesau F, Jannin S, Konter JA, Hautle P, Wenckebach WT, Gruetter R, van der Klink JJ. Design and Performance of a DNP Prepolarizer Coupled to a Rodent MRI Scanner. Concepts Magn Reson, Part B. 2007; 31B:255–269.
28. Bornet A, Melzi R, Perez Linde AJ, Hautle P, van den Brandt B, Jannin S, Bodenhausen G. Boosting Dissolution Dynamic Nuclear Polarization by Cross Polarization. J Phys Chem Lett. 2013; 4(1):111–114. [PubMed: 26291221]
29. Morris GA, Freeman R. Enhancement of Nuclear Magnetic-Resonance Signals by Polarization Transfer. J Am Chem Soc. 1979; 101(3):760–762.
30. Pines A, Gibby MG, Waugh JS. Proton-Enhanced NMR of Dilute Spins in Solids. J Chem Phys. 1973; 59(2):569–590.
31. Hartmann SR, Hahn EL. Nuclear Double Resonance in Rotating Frame. Phys Rev. 1962; 128(5): 2042–2053.
32. Wind RA, Li L, Lock H, Maciel GE. Dynamic Nuclear Polarization in the Rotating Frame. J Magn Reson. 1988; 79:577–582.
33. Farrar CT, Hall DA, Gerfen GJ, Rosay M, Ardenkjaer-Larsen JH, Griffin RG. High-frequency dynamic nuclear polarization in the nuclear rotating frame. J Magn Reson. 2000; 144(1):134–141. [PubMed: 10783283]
34. Weis V, Bennati M, Rosay M, Griffin RG. Solid effect in the electron spin dressed state: A new approach for dynamic nuclear polarization. J Chem Phys. 2000; 113:6795.
35. Weis V, Griffin RG. Electron-nuclear cross polarization. Solid State Nucl Magn Reson. 2006; 29(1–3):66–78. [PubMed: 16298515]
36. Brill AS. Intramolecular dynamic nuclear polarization via electron-nuclear double resonance. Phys Rev A: At, Mol, Opt Phys. 2002; 66:043405.
37. Morley GW, van Tol J, Ardavan A, Porfyrakis K, Zhang J, Briggs GA. Efficient dynamic nuclear polarization at high magnetic fields. Phys Rev Lett. 2007; 98(22):220501. [PubMed: 17677824]
38. Schuch H, Harris CB. Optically Detected Spin Locking of Zero Field Electronic Triplet States and Cross Relaxation in the Rotating Frame. Z Naturforsch, A: Phys Sci. 1975; 30:361–371.
39. Brunner H, Fritsch RH, Hausser KH. Cross Polarization in Electron Nuclear Double Resonance by Satisfying the Hartmann-Hahn Condition. Z Naturforsch, A: Phys Sci. 1987; 42:1456–1457.
40. Henstra A, Dirksen P, Schmidt J, Wenckebach WT. Nuclear Spin Orientation via Electron Spin Locking. J Magn Reson. 1988; 77:389–393.

41. Reynhardt EC, High GL. Dynamic nuclear polarization of diamond. II. Nuclear orientation via electron spin-locking. J Chem Phys. 1998; 109:4100.
42. Can TV, Walish JJ, Swager TM, Griffin RG. Time domain DNP with the NOVEL sequence. J Chem Phys. 2015; 143(5):054201. [PubMed: 26254646]
43. Henstra A, Lin TS, Schmidt J, Wenckebach WT. High Dynamic Nuclear Polarization at Room Temperature. Chem Phys Lett. 1990; 165:6–10.
44. van den Heuvel DJ, Henstra A, Lin TS, Schmidt J, Wenckebach WT. Transient oscillations in pulsed dynamic nuclear polarization. Chem Phys Lett. 1992; 188:194–200.
45. Schmidt J, van den Heuvel DJ, Henstra A, Lin TS, Wenckebach WT. Polarizing nuclear spins via photo-excited triplet states. Isr J Chem. 1992; 32:165–172.
46. Eichhorn TR, Haag M, van den Brandt B, Hautle P, Wenckebach WT. High proton spin polarization with DNP using the triplet state of pentacene-d14. Chem Phys Lett. 2013; 555:296–299.
47. Eichhorn TR, Brandt Bvd, Hautle P, Henstra A, Wenckebach WT. Dynamic nuclear polarisation via the integrated solid effect II: experiments on naphthalene-h8 doped with pentacene-d14. Mol Phys. 2014; 112:1773–1782.
48. Tateishi K, Negoro M, Nishida S, Kagawa A, Morita Y, Kitagawa M. Room temperature hyperpolarization of nuclear spins in bulk. Proc Natl Acad Sci U S A. 2014; 111(21):7527–7530. [PubMed: 24821773]
49. Macho V, Stehlik D, Vieth HM. Spin coherence effects in the electron-nuclear polarization transfer process. Chem Phys Lett. 1991; 180:398–402.
50. van den Heuvel DJ, Schmidt J, Wenckebach WT. Polarizing proton spins by electron-spin locking of photo-excited triplet state molecules. Chem Phys. 1994; 187:365–372.
51. Henstra A, Dirksen P, Wenckebach WT. Enhanced Dynamic Nuclear Polarization by the Integrated Solid Effect. Phys Lett A. 1988; 134:134–136.
52. Matsumoto K, English S, Yoo J, Yamada K, Devasahayam N, Cook JA, Mitchell JB, Subramanian S, Krishna MC. Pharmacokinetics of a triarylmethyl-type paramagnetic spin probe used in EPR oximetry. Magn Reson Med. 2004; 52(4):885–92. [PubMed: 15389949]
53. Hall DA, Maus DC, Gerfen GJ, Inati SJ, Becerra LR, Dahlquist FW, Griffin RG. Polarization-Enhanced NMR Spectroscopy of Biomolecules in Frozen Solution. Science. 1997; 276:930–932. [PubMed: 9139651]
54. Song C, Hu KN, Joo CG, Swager TM, Griffin RG. TOTAPOL: A Biradical Polarizing Agent for Dynamic Nuclear Polarization Experiments in Aqueous Media. J Am Chem Soc. 2006; 128:11385–11390. [PubMed: 16939261]
55. van der Wel PCA, Hu KN, Lewandowski J, Griffin RG. Dynamic Nuclear Polarization of Amyloidogenic Peptide Nanocrystals: GNNQQNY, a Core Segment of the Yeast Prion Protein Sup35p. J Am Chem Soc. 2006; 128:10840–10846. [PubMed: 16910679]
56. Debelouchina GT, Bayro MJ, Fitzpatrick AW, Ladizhansky V, Colvin MT, Caporini MA, Jaroniec CP, Bajaj VS, Rosay M, Macphee CE, Vendruscolo M, Maas WE, Dobson CM, Griffin RG. Higher order amyloid fibril structure by MAS NMR and DNP spectroscopy. J Am Chem Soc. 2013; 135(51):19237–19247. [PubMed: 24304221]
57. Henstra A, Wenckebach WT. The theory of nuclear orientation via electron spin locking (NOVEL). Mol Phys. 2008; 106:859–871.
58. Bowman MK, Mailer C, Halpern HJ. The solution conformation of triarylmethyl radicals. J Magn Reson. 2005; 172:254–267. [PubMed: 15649753]
59. Trukhan SN, Yudanov VF, Tormyshev VM, Rogozhnikova OY, Trukhin DV, Bowman MK, Krzyaniak MD, Chen H, Martyanov ON. Hyperfine interactions of narrow-line trityl radical with solvent molecules. J Magn Reson. 2013; 233:29–36. [PubMed: 23722184]
60. Griffin RG. Solid State Nuclear Magnetic Resonance of Lipid Bilayers. Methods Enzymol. 1981; 72:108–174. [PubMed: 7311829]
61. Muller L, Kumar A, Baumann T, Ernst RR. Transient Oscillations in NMR Cross-polarization Experiments in Solids. Phys Rev Lett. 1974; 32:1402–1406.
62. Fielding AJ, Carl PJ, Eaton GR, Eaton SS. Multifrequency EPR of Four Triarylmethyl Radicals. Appl Magn Reson. 2005; 28:231–238.

63. Marin-Montesinos I, Paniagua JC, Vilaseca M, Urtizberea A, Luis F, Feliz M, Lin F, Van Doorslaer S, Pons M. Self-assembled trityl radical capsules–implications for dynamic nuclear polarization. Phys Chem Chem Phys. 2015; 17(8):5785–5794. [PubMed: 25626422]

64. Bloembergen N. On the interaction of nuclear spins in a crystalline lattice. Physica. 1949; XV:386–426.

65. Jeffries, CD. Dynamic Nuclear Orientation. Interscience Publishers; New York: 1963.

66. Tegenfeldt J, Haeberlen U. Cross Polarization in Solids with Flip-Back of I-spin Magnetization. J Magn Reson. 1979; 36:453–457.

67. Lumata L, Kovacs Z, Sherry AD, Malloy C, Hill S, van Tol J, Yu L, Song L, Merritt ME. Electron spin resonance studies of trityl OX063 at a concentration optimal for DNP. Phys Chem Chem Phys. 2013; 15:9800–9807. [PubMed: 23676994]

68. Joye CD, Shapiro MA, Sirigiri JR, Temkin RJ. Demonstration of a 140-GHz 1-kW Confocal Gyro-Traveling-Wave Amplifier. IEEE Trans Electron Devices. 2009; 56(5):818–827. [PubMed: 20054451]

69. Nanni EA, Lewis SM, Shapiro MA, Griffin RG, Temkin RJ. Photonic-band-gap traveling-wave gyrotron amplifier. Phys Rev Lett. 2013; 111(23):235101. [PubMed: 24476286]

70. Rosay, MM. PhD Thesis. MIT; 2001.

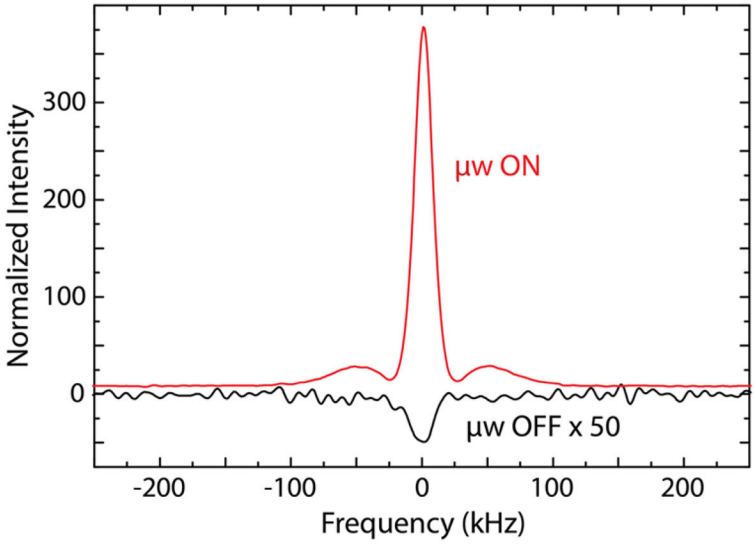

Figure 1.

^{1}H NMR signal enhancement by NOVEL DNP on a sample of d_8-glycerol/D_2O/H_2O (60/30/10 v/v/v) doped with 10.5 mM trityl OX063. The off-signal is an average of 4096 acquisitions, and the on-signal is an average of 256 acquisitions. Before each ^{1}H NMR acquisition, polarization is built up by repeating the electron spin lock at the NOVEL condition at a 1 kHz rate for 8 s. See also the Experimental Methods section.

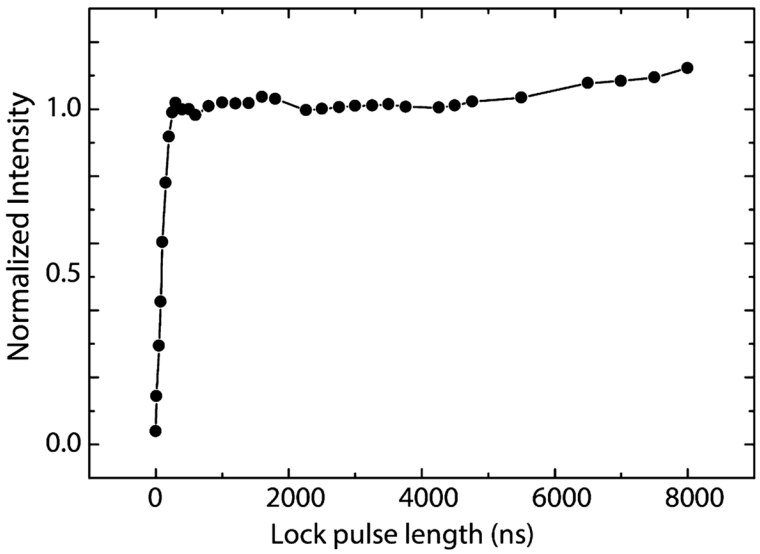

Figure 2.

^{1}H NMR signal enhancement by NOVEL DNP as a function of the length of the electron spin-locking pulse (mixing time). Each ^{1}H NMR spectrum is an average of 128 acquisitions. Before each ^{1}H NMR acquisition, polarization is built up by repeating the electron spin lock at the NOVEL condition at a 1 kHz rate for 2 s.

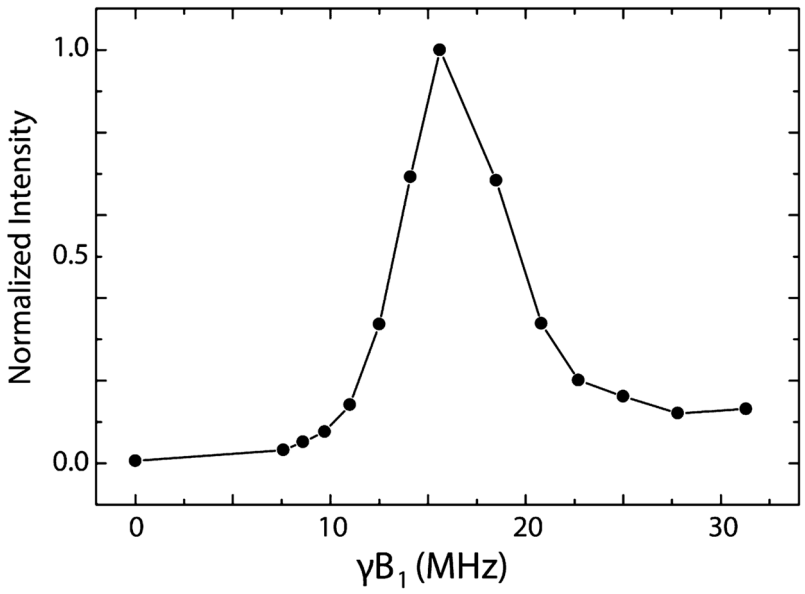

Figure 3.

Microwave field profile. ^{1}H NMR signal enhancement by NOVEL DNP as a function of the applied microwave field strength. The line connecting the dots is a guide to the eye. Each ^{1}H NMR spectrum is an average of 128 acquisitions. Before each ^{1}H NMR acquisition, polarization is built up by repeating the electron spin lock at the NOVEL condition at a 1 kHz rate for 2 s.

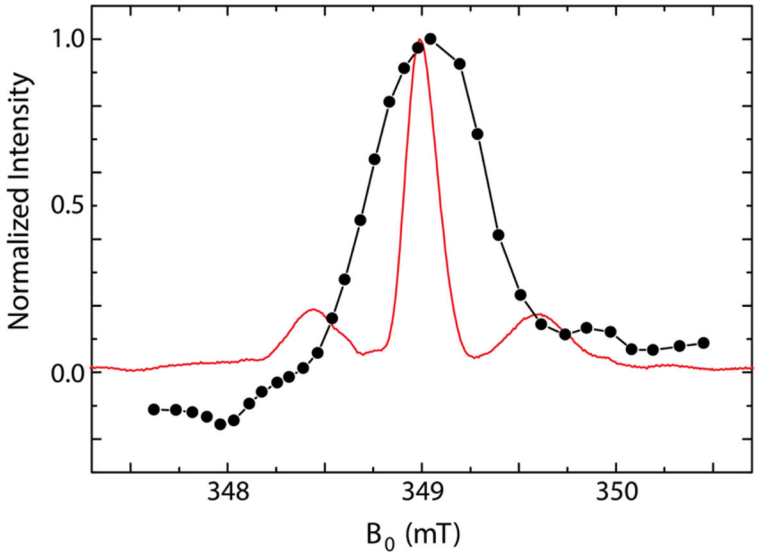

Figure 4.

Zeeman field profile. Field dependence of the ^{1}H NMR signal enhanced by NOVEL DNP (black dots, black line to guide the eye) together with the echo-detected EPR spectrum (red line) of a 10.5 mM trityl OX063 sample. The echo-detected EPR spectrum was recorded at a microwave frequency of 9.7837 GHz. The central peak occurs at 348.98 mT, which corresponds to a ^{1}H Larmor frequency of 14.859 MHz. To acquire the profile, we performed NOVEL experiments at this magnetic field, while the microwave frequency was swept. To compare the field profile to the echo-detected EPR spectrum we transformed the microwave frequency values to magnetic field values.

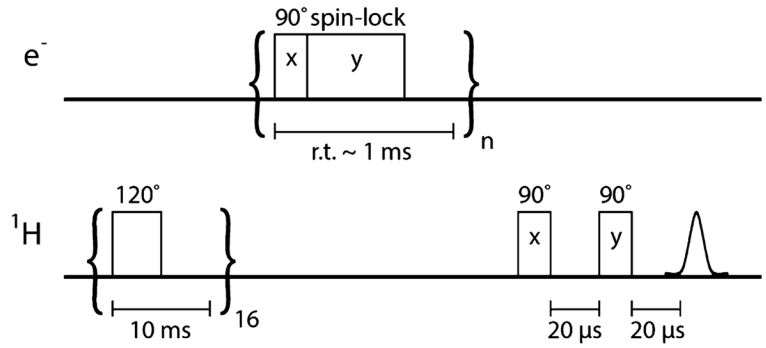

Scheme 1.
NOVEL Pulse Sequence